

PAPER • OPEN ACCESS

## Qubit state tomography in a superconducting circuit via weak measurements

To cite this article: Lupei Qin *et al* 2017 *New J. Phys.* **19** 033036

View the [article online](#) for updates and enhancements.

You may also like

- [Implementation of weak measurement amplification with the weak coherent light and optomechanical system](#)  
Gang Li and Wen Yang
- [Weak measurements of trajectories in quantum systems: classical, Bohmian and sum over paths](#)  
A Matzkin
- [Sequential measurements of non-commuting observables with quantum controlled interactions](#)  
Holger F Hofmann



## PAPER

## Qubit state tomography in a superconducting circuit via weak measurements

## OPEN ACCESS

## RECEIVED

7 December 2016

## REVISED

20 February 2017

## ACCEPTED FOR PUBLICATION

3 March 2017

## PUBLISHED

27 March 2017

Original content from this work may be used under the terms of the [Creative Commons Attribution 3.0 licence](#).

Any further distribution of this work must maintain attribution to the author(s) and the title of the work, journal citation and DOI.

Lupei Qin<sup>1</sup>, Luting Xu<sup>1</sup>, Wei Feng<sup>2</sup> and Xin-Qi Li<sup>1</sup><sup>1</sup> Center for Advanced Quantum Studies and Department of Physics, Beijing Normal University, Beijing 100875, People's Republic of China<sup>2</sup> Department of Physics, Tianjin University, Tianjin 300072, People's Republic of ChinaE-mail: [lixinqi@bnu.edu.cn](mailto:lixinqi@bnu.edu.cn)

Keywords: quantum weak measurement, weak value, state tomography

## Abstract

In this work we present a study on a new scheme for measuring the qubit state in a circuit quantum electrodynamics (QED) system, based on weak measurement and the concept of weak value. To be applicable under generic parameter conditions, our formulation and analysis are carried out for finite-strength weak measurement, and in particular beyond the bad-cavity and weak-response limits. The proposed study is accessible to present state-of-the-art circuit QED experiments.

## 1. Introduction

In quantum mechanics, the state of a single system (e.g., a single particle) is described by a wavefunction, which differs drastically from its description in classical mechanics. For all practical applications, the wavefunction works as tool for calculating the outcomes of experiments, while the underlying physics remains unclear. It is well known that the wavefunction cannot be determined via a single shot measurement [1]. However, with the advent of quantum information science and technology, experimental manipulation and determination of the wavefunction have become extremely important.

In order to determine the wavefunction, the standard method is based on projective strong measurement where the wavefunction is fully collapsed, and this has been termed *quantum state tomography* [2–9]. An alternative, new scheme, proposed and implemented very recently [10–15], is based on a different idea of sequentially measuring two complementary variables of the system [16–27]. The first measurement is weak and the second one is strong (projective). The weak measurement (each single one) gets minor information, makes little disturbance and does not collapse the state. The second, projective measurement plays a role of post-selection.

The key point is that, in this new scheme, it is the superposed *complex amplitudes* in the wavefunction (but not the *probabilities*) that are extracted *directly* from the single round average of the post-selected data of the first weak measurements. Under this sort of joint measurement, the full (complex) information of the wavefunction is encoded in the shift of the pointer in the measurement apparatus, in terms of the weak value (WV) introduced by Aharonov, Albert and Vaidman (AAV) nearly 30 years ago, given by [16]

$$A_w = \frac{\langle \psi_f | \hat{A} | \psi_i \rangle}{\langle \psi_f | \psi_i \rangle}, \quad (1)$$

where  $|\psi_i\rangle$  and  $|\psi_f\rangle$  are, respectively, in the context of state tomography, the state to be determined and the state for post-selection.  $\hat{A}$  is the weakly observed quantity. Recent experiments applying this method have been carried out to measure the photon's transverse wavefunction (a task not previously accomplished by any method) [10], the photon's polarization state [12, 13] and the high-dimensional orbital angular momentum state of the photon [14, 15].

The weak measurement is at the heart of this scheme, while it has also been an extensive research topic in recent years [28–37], particularly in the superconducting circuit quantum electrodynamics (cQED) system. In this work, we present an analysis of the weak-value-based scheme for qubit state tomography in the cQED

system. In order to apply to generic parameter conditions, our study will focus on the *finite strength* of weak measurement [38, 39]. This goes beyond the usual limit of vanishing strength, and thus results in a generalized pre- and post-selection (PPS) average, rather than the original AAV WV, as the shift of the pointer in the apparatus. Moreover, very recent research has shown that stronger finite-strength measurement can give a better result in state tomography [40], while some efforts are devoted to developing new schemes of dispersive readout [41–43], which go beyond the standard approach used in the state-of-the-art experiments [28–32, 35–37] and in our present work. To extract the AAV WV from the PPS average (raw signal), we propose to apply the analytic formula derived for the homodyne measurement in circuit QED [39]. By varying the phase of the local oscillator (LO), one can easily extract the complex weak value and determine the complex wavefunction by applying a simple iterative algorithm. For the first time, we also obtain an analytic result for the PPS average beyond the bad-cavity and weak-response limits, and demonstrate how to reliably determine the qubit state in this regime.

## 2. Methods

### 2.1. Measurement current and rates

The cQED system was originally described by the well-known Jaynes–Cummings model [28]. In the dispersive regime [28], i.e., with the detuning between the cavity frequency ( $\omega_r$ ) and qubit energy ( $\omega_q$ ) being much larger than the coupling strength  $g$ , the cQED system can be described by the Hamiltonian [28]

$$H_{\text{eff}} = \Delta_r a^\dagger a + \frac{\tilde{\omega}_q}{2} \sigma_z + \chi a^\dagger a \sigma_z + (\epsilon_m^* a + \epsilon_m a^\dagger), \quad (2)$$

where  $\Delta_r = \omega_r - \omega_m$  arises from the fact that this Hamiltonian is expressed in the rotating frame with the microwave drive frequency ( $\omega_m$ ). The transition frequency of the qubit reads  $\tilde{\omega}_q = \omega_q + \chi$ , which is modified by a dispersive shift  $\chi = g^2/\Delta$ , with  $\Delta = \omega_r - \omega_q$ . In equation (2),  $a^\dagger$  ( $a$ ) and  $\sigma_z$  are respectively the creation (annihilation) operator of the cavity photon and the quasi-spin (Pauli matrix) of the qubit.  $\epsilon_m$  is the microwave drive amplitude applied to the cavity.

The dispersive coupling characterized by the third term in the above Hamiltonian allows for a homodyne measurement with output current given by [44]

$$I(t) = -\sqrt{\Gamma_{ci}(t)} \langle \sigma_z \rangle + \xi(t), \quad (3)$$

where  $\xi(t)$  is a Gaussian white noise originating from fundamental quantum jumps during the measurement. This expression for the current was obtained in the absence of qubit rotation and by eliminating the cavity degrees of freedom (the so-called polaron transformation) [44]. In a bit more detail,  $\Gamma_{ci}(t)$  is the *coherent information* gain rate of measurement given by [44]

$$\Gamma_{ci}(t) = \kappa |\beta(t)|^2 \cos^2(\varphi - \theta_\beta), \quad (4)$$

where  $\varphi$  is the LO's phase in the homodyne measurement,  $\kappa$  is the leakage rate of the cavity photons, and  $\beta(t) = \alpha_2(t) - \alpha_1(t) \equiv |\beta(t)|e^{i\theta_\beta}$  with  $\alpha_1(t)$  and  $\alpha_2(t)$  being the cavity fields associated with the qubit states  $|1\rangle$  and  $|2\rangle$ , respectively.

In addition to the information gain rate  $\Gamma_{ci}$ , there exists as well a *no-information* back-action rate, which reads [44]

$$\Gamma_{ba}(t) = \kappa |\beta(t)|^2 \sin^2(\varphi - \theta_\beta). \quad (5)$$

To understand the physical meaning, let us consider the stochastic evolution of qubit state  $c_1(t)|1\rangle + c_2(t)|2\rangle$ , conditioned on measurement records in a single realization. The rate  $\Gamma_{ci}$  appearing in equation (3) is associated with *the attempt to distinguish the qubit basis states (information gain)*, which causes a change in probability between  $|1\rangle$  and  $|2\rangle$  conditioned on the measurement record, together with a relative phase change between them that conserves the quantum purity of the superposed state—this actually corresponds to the term ‘coherent information gain’. Unlike the information gain rate, the rate  $\Gamma_{ba}$  is only related to phase fluctuation between  $|1\rangle$  and  $|2\rangle$  (no change in probability). The sum of  $\Gamma_{ci}$  and  $\Gamma_{ba}$ ,  $\Gamma_m = \Gamma_{ci} + \Gamma_{ba}$ , gives the total measurement rate. Differing somehow from  $\Gamma_m$ , the overall decoherence rate is given by [44]

$$\Gamma_d(t) = 4\chi \text{Im}[\alpha_1(t)\alpha_2^*(t)], \quad (6)$$

as a result of tracing the cavity degrees of freedom from the whole entangled qubit-cavity state. An interesting point is that  $\Gamma_m$  is not necessarily equal to  $\Gamma_d$ , owing to certain ‘information loss’. It is only for ideal (quantum limited) measurement that  $\Gamma_m = \Gamma_d$  and the single quantum trajectory is a quantum-mechanically pure state.

### 2.2. Quantum Bayesian rule

Conditioned on the output currents, equation (3), one can faithfully keep track of the stochastic evolution of the qubit state. In order to get analytic expression for the PPS average, rather than the equation for the quantum

trajectory, we apply alternatively the quantum Bayesian rule (BR) [45–48]. Using the output currents during  $(0, t_m)$ , we update first the diagonal elements  $\rho_{jj}$  ( $j = 1, 2$ ) of the qubit state (density matrix) [47, 48]

$$\rho_{jj}(t_m) = \rho_{jj}(0) P_j(t_m) / \mathcal{N}(t_m), \quad (7)$$

where  $\mathcal{N}(t_m) = \sum_{j=1,2} \rho_{jj}(0) P_j(t_m)$ . This result simply follows the standard Bayes formula, and the *functional* distribution of current reads [48]

$$P_{1(2)}(t_m) = \frac{1}{\mathcal{N}_I} \exp \{ -\langle [I(t) - \bar{I}_{1(2)}(t)]^2 \rangle_{t_m} / (2V) \}, \quad (8)$$

where  $\bar{I}_{1(2)}(t) = \mp \sqrt{\Gamma_{ci}(t)}$  and  $\langle \cdot \rangle_{t_m} = (t_m)^{-1} \int_0^{t_m} dt \langle \cdot \rangle$ .  $V = 1/t_m$  is the distribution variance, and  $\mathcal{N}_I$  is the normalization factor of the distribution probability (to be canceled from the numerator and denominator of the Bayes formula). Note that equation (8) differs from our usual knowledge. According to the *central limit theorem*, corresponding to  $|1\rangle$  and  $|2\rangle$ , the averaged stochastic current,  $I_m = (t_m)^{-1} \int_0^{t_m} dt I(t)$ , should respectively be centred at  $\bar{I}_{1(2)} = \mp (t_m)^{-1} \int_0^{t_m} dt \sqrt{\Gamma_{ci}(t)}$  and satisfy the standard Gaussian distribution

$$P_{1(2)}(t_m) = (2\pi V)^{-1/2} \exp [-(I_m - \bar{I}_{1(2)})^2 / (2V)]. \quad (9)$$

In [48], we have demonstrated that this ‘standard’ result is valid only for a time-independent rate  $\Gamma_{ci}$ , in equation (3).

Secondly, we update the off-diagonal elements as follows:

$$\rho_{12}(t_m) = \rho_{12}(0) [\sqrt{P_1(t_m)P_2(t_m)} / \mathcal{N}(t_m)] D(t_m) \exp \{ -i[\Phi_1(t_m) + \Phi_2(t_m)] \}. \quad (10)$$

Compared to the original simple BR [45], a couple of correction factors appear in this result, specifically given by [47, 48]

$$D(t_m) = \exp \left\{ -\int_0^{t_m} dt [\Gamma_d(t) - \Gamma_m(t)] / 2 \right\}, \quad (11a)$$

$$\Phi_1(t_m) = \int_0^{t_m} dt \tilde{\Omega}_q(t), \quad (11b)$$

$$\Phi_2(t_m) = -\int_0^{t_m} dt \sqrt{\Gamma_{ba}(t)} I(t). \quad (11c)$$

Here we have introduced  $\tilde{\Omega}_q(t) = \omega_q + \chi + B(t)$ , i.e., the bare qubit energy  $\omega_q$  is renormalized by the dispersive shift  $\chi$  and the shift induced by the ac Stark effect,  $B(t) = 2\chi \text{Re}[\alpha_1(t)\alpha_2^*(t)]$ . Briefly speaking, the purity degradation factor  $D(t_m)$  is a result of non-ideality (information loss) in the measurement, while the two phase factors  $e^{-i\Phi_1(t_m)}$  and  $e^{-i\Phi_2(t_m)}$  result, respectively, from the dynamic ac Stark effect and the no-information back-action.

### 2.3. PPS average in the bad-cavity and weak-response limits

In experiments the cQED system is usually prepared in the bad-cavity and weak-response limits. In this case, the cavity field evolves to a stationary state on a timescale much shorter than the measurement time. One can thus carry out the ac Stark shift and all the rates using the *stationary* coherent-state fields of the cavity,  $\bar{\alpha}_1$  and  $\bar{\alpha}_2$ , which read [47]

$$\bar{\alpha}_{1(2)} = -i\epsilon_m / [-i(\Delta_r \pm \chi) + \kappa/2], \quad (12)$$

where  $\Delta_r = \omega_m - \omega_r$  is the offset of the measurement and cavity frequencies. For instance, in the bad-cavity and weak-response limits, we obtain the stationary  $B(t)$  as  $B \simeq 2\chi\bar{n}$ , where  $\bar{n} = |\bar{\alpha}|^2$  and  $\bar{\alpha} = -i\epsilon_m / (\kappa/2)$ , which recovers the standard ac Stark shift. Also, a resonant drive ( $\omega_m = \omega_r$ ) results in  $\theta_\beta = 0$ .

Now let us consider the weak value for finite-strength measurement. For simplicity, we denote the measurement result as  $x \equiv I_m = (t_m)^{-1} \int_0^{t_m} dt I(t)$ , and  $\bar{x}_j \equiv \bar{I}_j = (-1)^j \sqrt{\Gamma_{ci}}$ . In the same spirit as the AAV WV for an infinitesimal strength of measurement, we employ the following PPS average as a definition for the WV associated with finite-strength measurement [20, 38, 39]:

$${}_f \langle x \rangle_i = \frac{\int dx x P_{\psi_i}(x) P_x(\psi_f)}{\int dx P_{\psi_i}(x) P_x(\psi_f)}. \quad (13)$$

$P_{\psi_i}(x)$  is the distribution probability of the measurement outcomes associated with the pre-selected state  $|\psi_i\rangle$ , before the post-selection using  $|\psi_f\rangle$ .  $P_x(\psi_f)$  is the post-selection probability given by  $P_x(\psi_f) = \langle \psi_f | \tilde{\rho}(x) | \psi_f \rangle$ , by applying the quantum BR to update the state from  $\rho_i$  to  $\tilde{\rho}(x)$ , based on the measurement outcome  $x$ . After some algebra, we obtain [39]

$$f\langle x \rangle_i = -\frac{\epsilon_1 \operatorname{Re}(\sigma_w^z) + \epsilon_2 \operatorname{Im}(\sigma_w^z)}{1 + \mathcal{G}(|\sigma_w^z|^2 - 1)}, \quad (14)$$

where  $\epsilon_1 = \sqrt{\Gamma_{ci}}$ ,  $\epsilon_2 = \sqrt{\Gamma_{ba}} e^{-\Gamma_d t_m}$  and  $\mathcal{G} = (1 - e^{-\Gamma_d t_m})/2$ . In this result, the AAV WV is slightly modified as

$$\sigma_w^z = \frac{\langle \psi_f | \sigma_z | \tilde{\psi}_i \rangle}{\langle \psi_f | \tilde{\psi}_i \rangle}, \quad (15)$$

where  $|\tilde{\psi}_i\rangle$  differs from the initial state  $|\psi_i\rangle = c_1|1\rangle + c_2|2\rangle$  by a phase factor as  $|\tilde{\psi}_i\rangle = c_1 e^{-i\tilde{\Omega}_q t_m}|1\rangle + c_2|2\rangle$ .

We see that, by tuning the LO phase  $\varphi$  based on equation (14), one can conveniently obtain the real and imaginary parts of  $\tilde{\sigma}_w^z$ , from which an efficient technique of state tomography can be developed for finite-strength measurement.

In experiments, the PPS average  $f\langle x \rangle_i$ , or the *meter's shift* in other words, is the *sub-ensemble* average of output currents, post-selected from the records of the first stage of weak (partial collapse) measurement. In practice, one should keep and average only those 'x' data that are followed by successful post-selection of  $|\psi\rangle_f$ . To generate this post-selection for each trajectory, one may rotate the qubit state (quite arbitrarily) at the moment  $t_m$ , and determine  $|\psi\rangle_f$  as the rotated version of the former basis state  $|1\rangle$ . This procedure actually defines a new basis for the subsequent post-selection, i.e., with  $|1\rangle$  corresponding to  $|\psi\rangle_f$ . We may mention that this method of obtaining  $f\langle x \rangle_i$  is not affected by the measurement strength. After getting  $f\langle x \rangle_i$ , the AAV WV can be easily extracted from equation (14).

#### 2.4. Beyond bad-cavity and weak-response limits

Following the same definition of the PPS average, equation (13), we have

$$f\langle x \rangle_i = \frac{\int \mathcal{D}[I(t)] x[I(t)] P_{\psi_i}(\{I(t)\}) P_{\{I(t)\}}(\psi_f)}{\int \mathcal{D}[I(t)] P_{\psi_i}(\{I(t)\}) P_{\{I(t)\}}(\psi_f)} \equiv \frac{M_1}{M_2}, \quad (16)$$

where  $x[I(t)] = (t_m)^{-1} \int_0^{t_m} I(t) dt$ , and the two probability distribution functionals read

$$\begin{aligned} P_{\psi_i}(\{I(t)\}) &= \rho_{11}(0)P_1(t_m) + \rho_{22}(0)P_2(t_m), \\ P_{\{I(t)\}}(\psi_f) &= \tilde{\rho}_{11}\rho_{f11} + \tilde{\rho}_{22}\rho_{f22} + \tilde{\rho}_{12}\rho_{f21} + \tilde{\rho}_{21}\rho_{f12}. \end{aligned}$$

Here we have denoted the Bayesian updated state by  $\tilde{\rho} = \tilde{\rho}(x) = \tilde{\rho}(\{I(t)\})$ . The probabilities  $P_{1,2}(t_m)$  follow equation (8), being *functionals* of the current record  $\{I(t) | t \in [0, t_m]\}$ . In equation (16), involved in both the numerator and denominator is the functional (or 'path') integral,  $\int \mathcal{D}[I(t)](\dots)$ , which means summing all the possible currents of the measurement. By means of the Gaussian path-integral method, calculation of equation (16) is straightforward. We obtain

$$\begin{aligned} M_1 &= -\left(\int_0^{t_m} \sqrt{\Gamma_{ci}(t)} dt\right) (\rho_{11}\rho_{f11} - \rho_{22}\rho_{f22}) + \left(\int_0^{t_m} \sqrt{\Gamma_{ba}(t)} dt\right) e^{-\int_0^{t_m} \Gamma_d(t) dt} \\ &\quad \times 2 \operatorname{Im}(\rho_{21}\rho_{f12} e^{i\int_0^{t_m} \tilde{\Omega}(t) dt}), \end{aligned} \quad (17)$$

$$M_2 = \rho_{11}\rho_{f11} + \rho_{22}\rho_{f22} + \left(e^{-\int_0^{t_m} \Gamma_d(t) dt}\right) \times 2 \operatorname{Re}(\rho_{21}\rho_{f12} e^{i\int_0^{t_m} \tilde{\Omega}(t) dt}). \quad (18)$$

Reorganizing this result further in terms of the AAV WV form, we find that the same expression as equation (14) can be obtained, with only several parameters modified as

$$\epsilon_1 = \int_0^{t_m} \sqrt{\Gamma_{ci}(t)} dt, \quad \epsilon_2 = \int_0^{t_m} \sqrt{\Gamma_{ba}(t)} dt e^{-\int_0^{t_m} \Gamma_d(t) dt}, \quad \mathcal{G} = (1 - e^{-\int_0^{t_m} \Gamma_d(t) dt})/2. \quad (19)$$

The AAV WV of equation (15) is now modified by replacing the initial state  $|\psi_i\rangle$  with  $|\tilde{\psi}_i\rangle = c_1 e^{-i\Phi_1(t_m)}|1\rangle + c_2|2\rangle$ .  $\Phi_1(t_m)$  is given by equation (11b).

Actually, the above weak-value formalism that results in (17) and (18) can be related to the past quantum state (PQS) formalism proposed recently [33–37], if we replace the density matrix  $\rho_{ij} = \langle i|\rho_f|j\rangle$  by the PQS *Effect Matrix*  $E_{ij} = \langle i|\hat{E}|j\rangle$ . The PQS formalism generalized the post-selection in the WV problem to successive continuous measurements characterized by the positive-operator valued measure (POVM) operator  $\hat{E}$ , which in general does not collapse the superposed state of a qubit. However, for the purpose of state tomography, the post-continuous measurement in PQS is harder to repeat than the post-selection in the weak value because of its highly stochastic nature. Therefore the PQS should be hard to apply to the problem of state tomography.

## 2.5. Numerical methods

From equation (14) we see that, in the *weak limit* of measurement (the linear response regime), we may approximate the denominator by unity (neglecting the second term). In this case one can obtain  $\text{Re}(\sigma_w^z)$  and  $\text{Im}(\sigma_w^z)$  from the PPS average of currents by choosing, respectively, the LO's phase  $\varphi = 0$  and  $\pi/2$ . In the more general case (the nonlinear response regime), the full denominator of equation (14) should be taken into account. In this case one can extract  $\text{Re}(\sigma_w^z)$  and  $\text{Im}(\sigma_w^z)$  by applying an *iterative* algorithm. That is, first, set trial values for the real and imaginary parts of the AAV WV through

$$\text{Re}(\sigma_w^z) \Leftarrow -\langle f(x)_i / \epsilon_1 \rangle|_{\varphi=0}, \quad \text{Im}(\sigma_w^z) \Leftarrow -\langle f(x)_i / \epsilon_2 \rangle|_{\varphi=\pi/2}.$$

Then, iteratively evaluate equation (14) several times until convergence is reached. In our numerical example illustrated in the next section, we found that this iterative approach is always efficient. The reason for applying this procedure is that there is a '± sign' problem when solving the AAV WV from the *quadratic* equation (14). An alternative method to overcome this problem is not solving for the AAV WV from equation (14), but solving for the unknown density matrix elements  $\rho_{ij}$  directly from the *linear* equations (16)–(18).

Regarding the accuracy of the AAV WV extracted, we find that, by simulating  $10^6$  trajectories, an accuracy of 0.5% can be achieved for  $\varphi = 0$ , which decreases to 3% for  $\varphi = \pi/2$ . The reason is that, in the latter case, the component related to information gain (the first term) in equation (3) vanishes, thus resulting in stronger fluctuations of the output currents. In practice, one may choose  $\varphi = \pi/4$  rather than  $\pi/2$ . Using equation (14),  $\text{Re}(\sigma_w^z)$  and  $\text{Im}(\sigma_w^z)$  can be easily extracted as well. For this choice, the same accuracy as for  $\varphi = 0$  can be achieved.

With the knowledge of  $\text{Re}(\sigma_w^z)$  and  $\text{Im}(\sigma_w^z)$ , based on equation (15), one can *directly* determine the unknown state,  $|\psi_i\rangle = c_1|1\rangle + c_2|2\rangle$ , as follows. Note that, owing to the dynamic ac Stark effect, the wavefunction involved in the AAV WV is actually 'modified' as  $|\tilde{\psi}_i\rangle = c_1 e^{-i\Phi_1(t_m)}|1\rangle + c_2|2\rangle$ . Up to a normalization factor, we rewrite this unknown state as

$$|\tilde{\psi}_i\rangle = |1\rangle + \tilde{c}|2\rangle, \quad (20)$$

where  $\tilde{c} = (c_2/c_1)e^{i\Phi_1}$ . For a given post-selection state  $|\psi_f\rangle = b_1|1\rangle + b_2|2\rangle$ , the AAV WV can be expressed as

$$\sigma_w^z = \frac{b_1^* - b_2^* \tilde{c}}{b_1^* + b_2^* \tilde{c}}. \quad (21)$$

From this result, we obtain

$$\tilde{c} = \left( \frac{1 - \sigma_w^z}{1 + \sigma_w^z} \right) \left( \frac{b_1}{b_2} \right)^* \equiv r e^{i\tilde{\theta}}, \quad (22)$$

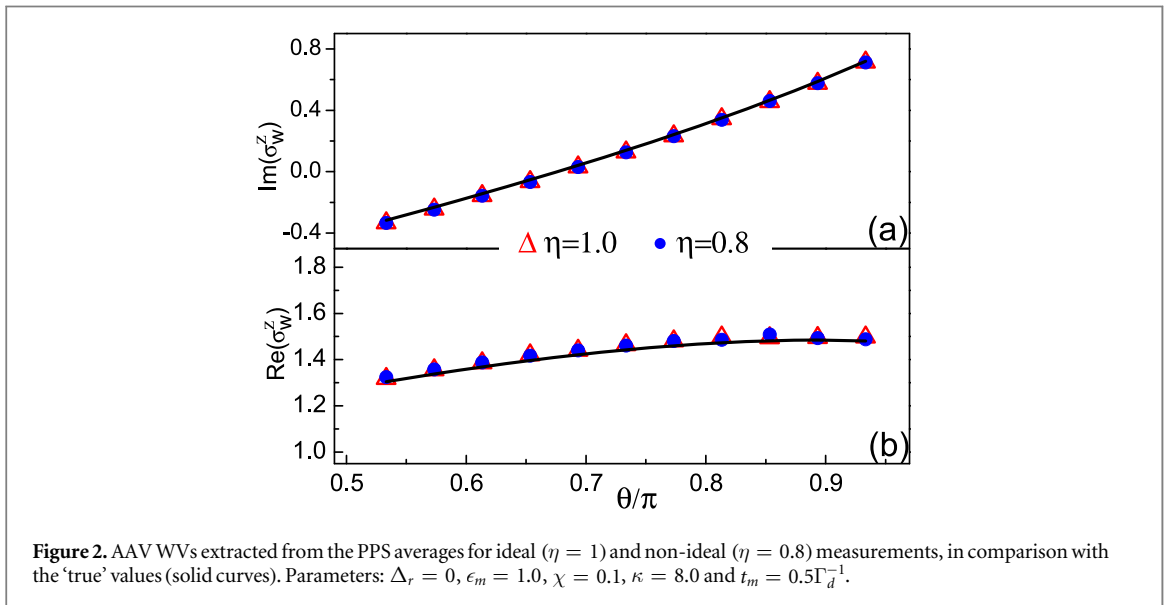
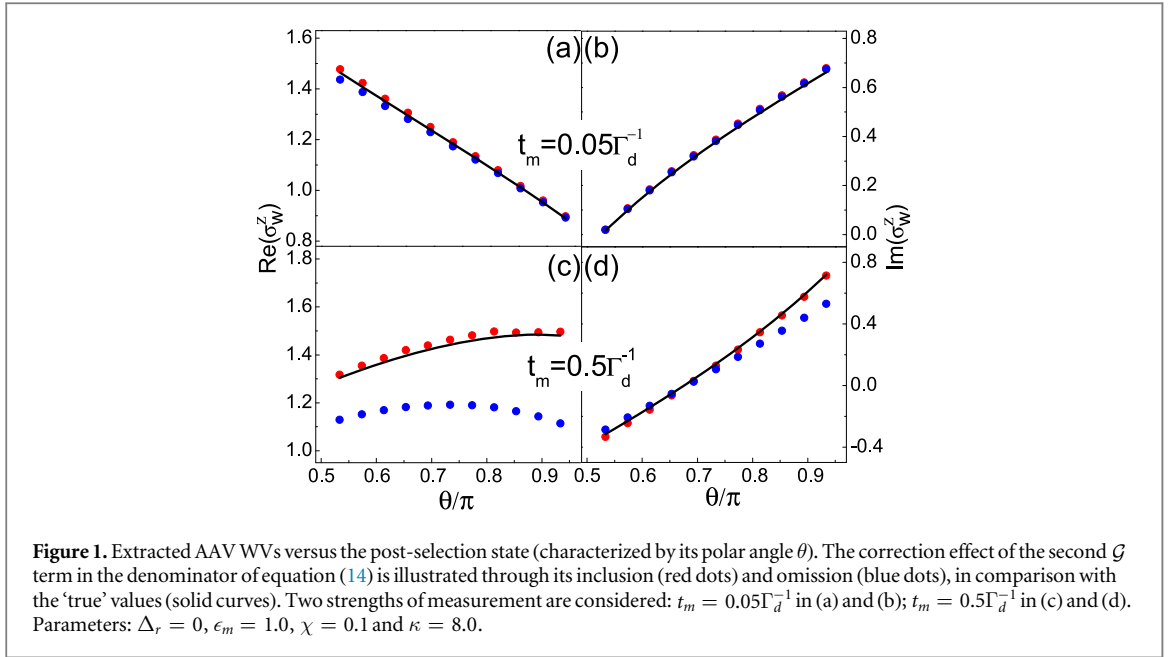
which fully characterizes the unknown state  $|\psi_i\rangle$  by noting that  $c_2/c_1 = r e^{i(\tilde{\theta}-\Phi_1)}$ .

## 3. Results

In all the simulations, we consider measurement under resonant driving, which corresponds to  $\Delta_r = \omega_r - \omega_m = 0$  where  $\omega_r$  and  $\omega_m$  are, respectively, the cavity frequency and the frequency of the measuring microwave. Corresponding to the experiments [29–32] and the associated theory [46], the results in figures 1–4 apply in the bad-cavity and weak-response regime. In an arbitrary system of units, we denote the strength of the microwave drive as  $\epsilon_m = 1.0$ , then set  $\kappa = 8$  and  $\chi = 0.1$  under the bad-cavity and weak-coupling conditions. With this choice, one can estimate the average photon number in the cavity (in a steady state) as  $\bar{n} \simeq 0.006$ , from  $\bar{n} = |\alpha_0|^2$  and  $\alpha_0 = -i\epsilon_m/(\kappa/2)$ . This weak field in the cavity, together with the weak dispersive coupling  $\chi$ , defines also a regime of weak response (in the sense of the measurement signal to the qubit state). However, in figure 5 we display results beyond the bad-cavity and weak-response limits by setting  $\kappa = 2$  and keeping  $\epsilon_m$  and  $\kappa$  unchanged, which results in the average cavity photon number  $\bar{n} = 1.0$  in a steady state.

In the following results, we denote the unknown (to be determined) state as  $|\psi_i\rangle = \cos \frac{\theta_i}{2} |1\rangle + \sin \frac{\theta_i}{2} e^{-i\phi_i} |2\rangle$ , and 'secretly' assign  $\theta_i = \pi/3$  and  $\phi_i = 50\tilde{\Omega}_q$ . For the post-selection state  $|\psi_f\rangle$ , we only alter the polar angle  $\theta$  to illustrate the quality of tomography. In all cases, we run the polaron-transformed effective quantum trajectory equation [39, 44] to generate  $10^6$  PPS trajectories.

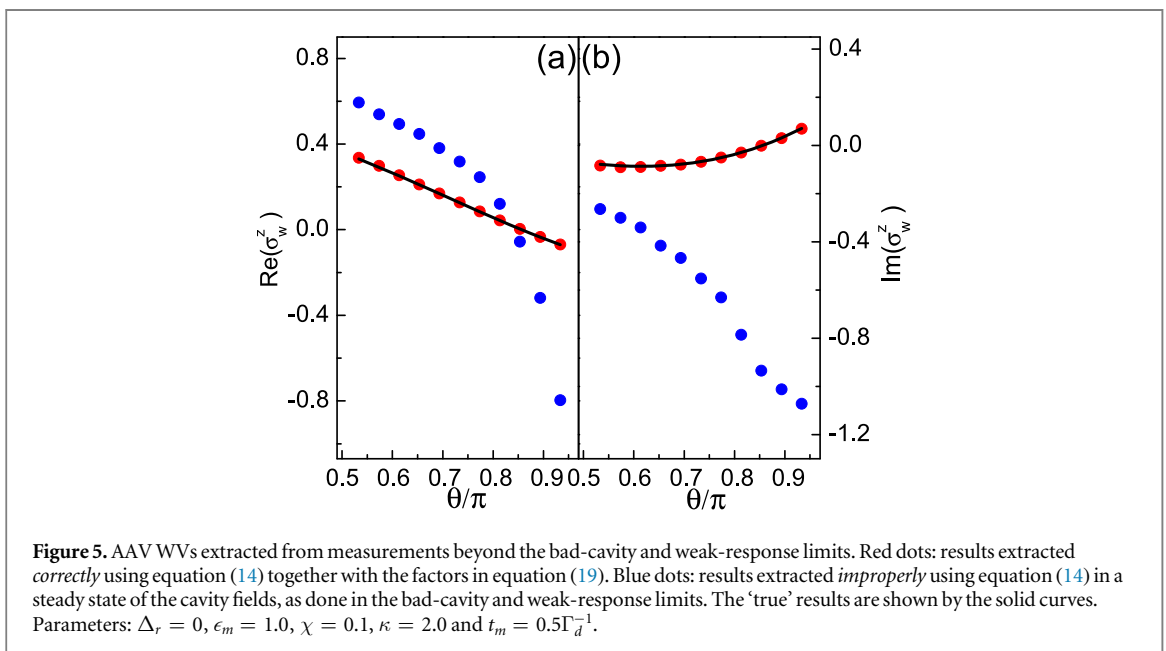
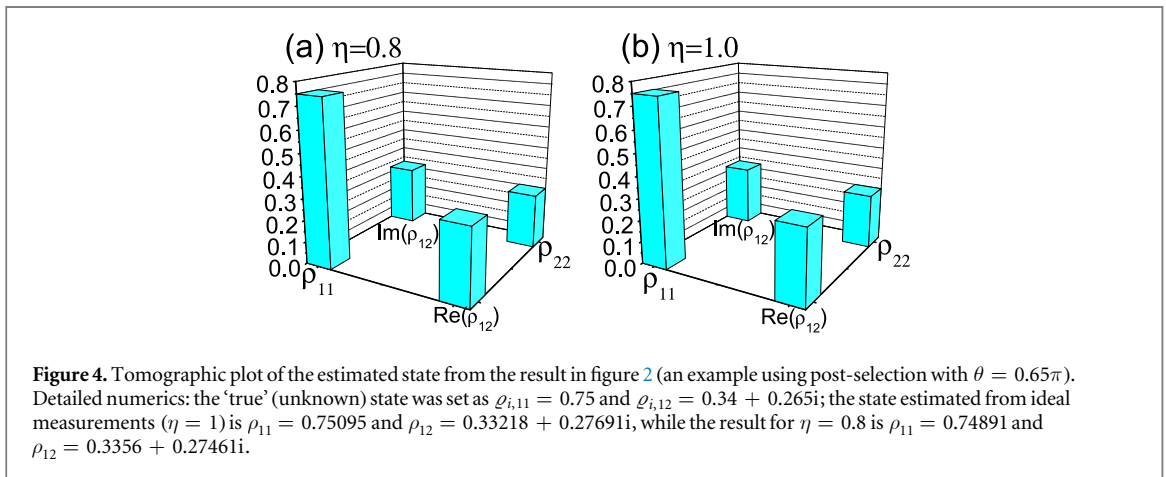
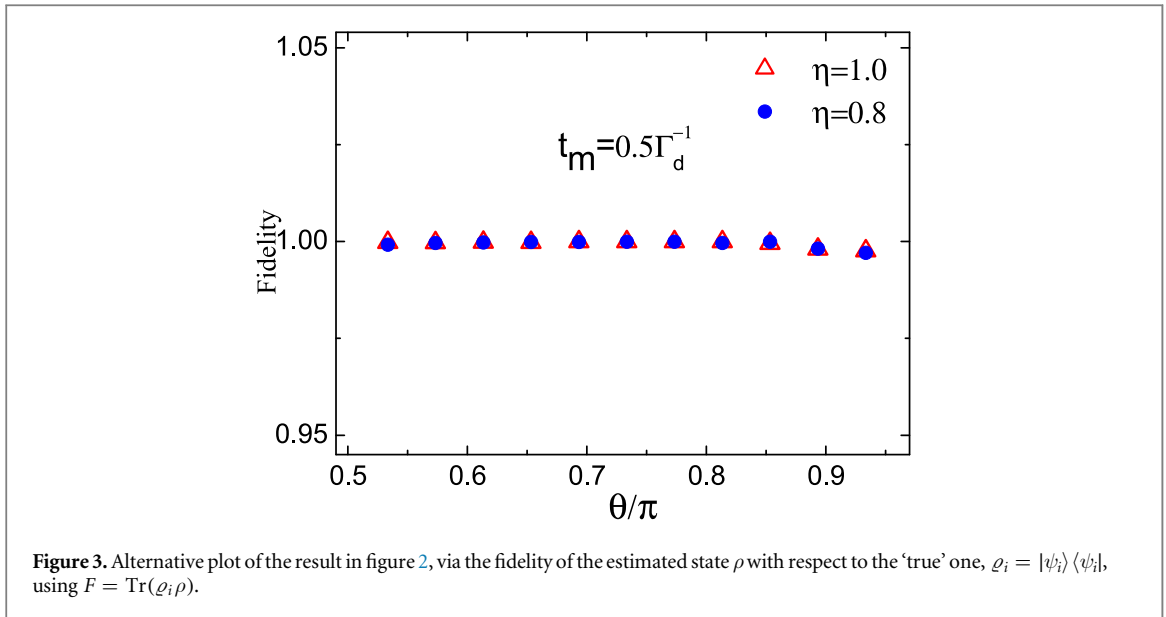
In figure 1 we display the extracted AAV WV against the post-selection state  $|\psi_f\rangle$ . Our main interest here is the correction effect of the second  $\mathcal{G}$  term in the denominator of equation (14). We thus simulate two strengths of measurement by choosing the measurement time  $t_m = 0.05\Gamma_d^{-1}$  for figures 1(a) and (b), and  $t_m = 0.5\Gamma_d^{-1}$  for (c) and (d). We compare the AAV WVs (the red and blue dots) extracted from equation (14) with the 'true' results (solid lines) calculated using equation (15) with the 'testing' state  $|\psi_i\rangle$ . The results shown by the red dots are extracted from the full formula of equation (14), while the blue dots are obtained by neglecting the second  $\mathcal{G}$



term in the denominator. We see that for vanishing strength of measurement, as shown in figures 1(a) and (b), the effect of the  $\mathcal{G}$  term is negligible. However, for a finite strength of measurement (figures 1(c) and (d)), one must take the  $\mathcal{G}$  term into account.

We now turn to investigate the possible influence of the quantum *efficiency* of the weak measurement on the present tomography method. Actually, the conventional scheme is rather less severely impacted by the quantum inefficiency, since many tomography experiments were successfully performed before the advent of efficient amplification. At first sight, the present scheme based on continuous weak measurement will be influenced by the quantum efficiency of the measurement, since quantum efficiency will affect state inference (e.g. the off-diagonal elements) conditioned on the measurement results, and thus affect the probability of success of post-selection. However, in our previous study [39], the weak values (PPS averages) of similar qubit measurements were found to be free from the quantum efficiency of the detector. Below, we illustrate numerically that, indeed, the present tomographic scheme is free from the quantum efficiency of the homodyne detection.

For the set-up of the present investigation, there are two main sources affecting the quantum efficiency of the measurement. One is the noise added in the signal amplification; the other is the photon loss during signal collection. However, both sources can be commonly characterized in theory by the parameter  $\eta$  (the quantum efficiency) [44, 46]. Within the Bayesian formalism, the inefficiency can be simply accounted for by inserting a



decoherence factor  $e^{-(1-\eta)\Gamma_m t}$  into the off-diagonal elements of the qubit state; when running the quantum trajectory equation [39, 44], one can simultaneously reduce the rates  $\Gamma_{ci}$  and  $\Gamma_{ba}$  by a factor ‘ $1 - \eta$ ’.

In figure 2 we compare the AAV WV extracted from the ideal measurement (red triangles, with  $\eta = 1$ ) with the result for efficiency  $\eta = 0.8$  (blue dots)<sup>3</sup>, while plotting both against the ‘true’ result (solid curve). Indeed, we find all three results in perfect agreement. In figure 3 we further display the fidelity of the estimated state  $\rho$  with respect to the ‘true’ one,  $\rho_i = |\psi_i\rangle\langle\psi_i|$ , using the fidelity definition  $F = \text{Tr}(\rho_i \rho)$ , while in figure 4 we characterize, for a specific example, the full state (diagonal and off-diagonal elements of the density matrix) in terms of the usual means of quantum state tomography. Through these results, we see that, indeed, the weak-value-associated scheme of quantum state tomography is free from the efficiency of quantum measurement.

Actually, this *efficiency-free* statement is from averaging a sufficient number of trajectories, which was implied in the analytic proof in [39] and in the above numerical demonstrations. For a limited measurement resource (limited size of trajectory ensemble), the small number of photons detected (owing to poor efficiency) will cause strong fluctuations and errors for state tomography. In practice, this problem can be partly overcome by increasing the driving power of the measuring microwave and properly enhancing the time of weak measurement (collecting more photons to yield the integrated current for the Bayesian inference). Our formulation, equation (14) together with (19), being valid for *finite-strength* measurement under broad parameter conditions, will be useful in solving this problem. This solving strategy is also supported by very recent research [40], which showed that stronger finite-strength measurement can give a better result for the weak-value-based tomographic scheme.

Finally, let us consider the situation beyond the bad-cavity and weak-response limits, and illustrate how to reliably extract the AAV WV and determine the qubit state. Actually, the basic requirement of the bad-cavity and weak-response limits is  $\kappa \gg \chi$  [47, 48]. Under this condition, the time-dependent factor in the cavity field dynamics [47, 48],  $e^{\pm i\chi t} e^{-\kappa t/2}$ , would become less important so that we can neglect the transient dynamics of the cavity field, and all the rates ( $\Gamma_d$ ,  $\Gamma_{ba}$  and  $\Gamma_{ci}$ ) can be treated as steady-state constants. Thus, we simply change  $\kappa = 8$  to  $\kappa = 2$  and keep all the other parameters the same as in figures 1–4. In this case, if we *improperly* use equation (14) with all the rates and the ac Stark shift determined by the steady-state cavity fields, as indicated by the blue dots in figure 5, the extracted AAV WV will suffer serious error from the ‘true’ result. However, if instead we combine equation (14) with the factors given by equation (19), satisfactory results can be obtained, as shown in figure 5 by the red dots. This ensures that the present scheme of state tomography can be applied beyond the bad-cavity and weak-response limits, if one properly applies equations (14) and (19).

## 4. Summary and discussions

We have presented a scheme for qubit state tomography in the superconducting circuit QED system, based on weak measurements and the associated quantum Bayesian approach. The Bayesian approach allows us to derive a compact expression for the PPS average, which encodes the full information of the AAV WV and makes the participation of its real and imaginary parts tunable by modulating the LO phase of the homodyne measurement. For the first time, we also obtained an analytic expression for the PPS average beyond the bad-cavity and weak-response limits, and demonstrated how to determine the qubit state in this regime.

It would be of interest in the circuit QED system to explore the direct scheme of state tomography for more complicated states, e.g., an entangled state of multiple qubits and a nontrivial state of cavity fields. We propose to leave these problems for future investigations.

We may conclude the present work with a few more remarks. (i) Compared with the conventional method of tomography, which measures separately the averages of  $\sigma_x$ ,  $\sigma_y$  and  $\sigma_z$  and thus needs precise orthogonal basis rotations, the weak-value-based scheme involves simpler (quite arbitrary) state rotation for the post-selection to encode the full complex information of the unknown state into a single PPS average. (ii) While the post-selection involves the discarding of data, this problem in state tomography is less severe than the amplifications based on a singular weak value. For state tomography, if the measured state is not severely orthogonal to the post-selection state, most data can survive in the post-selection. (iii) Comprehensive and quantitative assessment of the quality and efficiency of the new scheme against the conventional one is an open question worth further analysis by taking into account, for instance, the post-selection, the number of measurements, and the tolerance to imperfections (e.g. improper rotations, unfaithful measurements, etc).

<sup>3</sup> The efficiency of quantum measurement in circuit QED experiments is currently around 0.4–0.5, while further improvement is expected in the near future. In our simulation we assumed a modest efficiency  $\eta = 0.8$ . The important point is that the quantum efficiency does not affect the task of state tomography, which is actually guaranteed by two essential proofs: (i) Applying the quantum Bayesian rule, in [39], we analytically proved that the PPS average  $f(x)$  is free from  $\eta$ . (ii) In [48], even beyond the bad-cavity and weak-response limits, we analytically proved the equivalence between the Bayesian rule and the quantum trajectory equation for arbitrary  $\eta$ .

## Acknowledgments

This work was supported by the Major State '973' Project of China under No. 2012CB932704, the NNSF of China under Nos. 11675016 & 21421003, the Beijing NSF under No. 1164014 and the Fundamental Research Funds for Central Universities.

## References

- [1] Wootters W K and Zurek W H 1982 *Nature* **299** 802
- [2] Vogel K and Risken H 1989 *Phys. Rev. A* **40** 2847
- [3] Smithey D T, Beck M, Raymer M G and Faridani A 1993 *Phys. Rev. Lett.* **70** 1244
- [4] Breitenbach G, Schiller S and Mlynek J 1997 *Nature* **387** 471
- [5] White A G, James D F V, Eberhard P H and Kwiat P G 1999 *Phys. Rev. Lett.* **83** 3103
- [6] Hofheinz M et al 2009 *Nature* **459** 546
- [7] Teo Y S, Zhu H, Englert B-G, Rehacek J and Hradil Z 2011 *Phys. Rev. Lett.* **107** 020404
- [8] Zhu H and Englert B-G 2011 *Phys. Rev. A* **84** 022327
- [9] Zhu H 2014 *Phys. Rev. A* **90** 012115
- [10] Lundeen J S, Sutherland B, Patel A, Stewart C and Bamber C 2011 *Nature* **474** 188
- [11] Lundeen J S and Bamber C 2012 *Phys. Rev. Lett.* **108** 70402
- [12] Thekkadath G S, Giner L, Chalich Y, Horton M J, Banker J and Lundeen J S 2016 *Phys. Rev. Lett.* **117** 120401
- [13] Salvail J Z, Agnew M, Johnson A S, Bolduc E, Leach J and Boyd R W 2013 *Nat. Photon.* **7** 316
- [14] Malik M, Mirhosseini M, Lavery M P J, Leach J, Padgett M J and Boyd R W 2014 *Nat. Commun.* **5** 3115
- [15] Malik M and Boyd R W 2014 *Quantum Imaging Technologies* **37** 273
- [16] Aharonov Y, Albert D and Vaidman L 1988 *Phys. Rev. Lett.* **60** 1351
- [17] Duck I M, Stevenson P M and Sudarshan E C G 1989 *Phys. Rev. D* **40** 2112
- [18] Aharonov Y and Vaidman L 1990 *Phys. Rev. A* **41** 11
- [19] Ritchie N W M, Story J G and Hulet R G 1991 *Phys. Rev. Lett.* **66** 1107
- [20] Wiseman H 2002 *Phys. Rev. A* **65** 032111
- [21] Solli D R, McCormick C F, Chiao R Y, Popescu S and Hickmann J M 2004 *Phys. Rev. Lett.* **92** 043601
- [22] Johansen L 2004 *Phys. Rev. Lett.* **93** 120402
- [23] Pryde G J, O'Brien J L, White A G, Ralph T C and Wiseman H M 2005 *Phys. Rev. Lett.* **94** 220405
- [24] Hosten O and Kwiat P 2008 *Science* **319** 787
- [25] Dixon P B, Starling D J, Jordan A N and Howell J C 2009 *Phys. Rev. Lett.* **102** 173601
- [26] Kocsis S et al 2011 *Science* **332** 1170
- [27] Feizpour A, Xing X and Steinberg A M 2011 *Phys. Rev. Lett.* **107** 133603
- [28] Blais A, Huang R S, Wallraff A, Girvin S M and Schoelkopf R J 2004 *Phys. Rev. A* **69** 062320
- [29] Wallraff A, Schuster D I, Blais A, Frunzio L, Huang R S, Majer J, Kumar S, Girvin S M and Schoelkopf R J 2004 *Nature* **431** 162
- [30] Vijay R, Macklin C, Slichter D H, Weber S J, Murch K W, Naik R, Korotkov A N and Siddiqi I 2012 *Nature* **490** 77
- [31] Hatridge M et al 2013 *Science* **339** 178
- [32] Murch K W, Weber S J, Macklin C and Siddiqi I 2013 *Nature* **502** 211
- [33] Gammelmark S, Julsgaard B and Molmer K 2013 *Phys. Rev. Lett.* **111** 160401
- [34] Rybarczyk T et al 2015 *Phys. Rev. A* **91** 062116
- [35] Tan D, Weber S J, Siddiqi I, Molmer K and Murch K W 2015 *Phys. Rev. Lett.* **114** 090403
- [36] Greplova E, Molmer K and Andersen C K 2016 *Phys. Rev. A* **94** 042334
- [37] Tan D, Naghiloo M, Molmer K and Murch K W 2016 *Phys. Rev. A* **94** 050102
- [38] Williams N S and Jordan A N 2008 *Phys. Rev. Lett.* **100** 026804
- [39] Qin L, Liang P and Li X Q 2015 *Phys. Rev. A* **92** 012119
- [40] Vallone G and Dequal D 2016 *Phys. Rev. Lett.* **116** 040502
- [41] Didier N, Kamal A, Oliver W D, Blais A and Clerk A A 2015 *Phys. Rev. Lett.* **115** 093604
- [42] Didier N, Bourassa J and Blais A 2015 *Phys. Rev. Lett.* **115** 203601
- [43] McClure D T, Paik H, Bishop L S, Steffen M, Chow J M and Gambetta J M 2016 *Phys. Rev. Appl.* **5** 011001
- [44] Gambetta J, Blais A, Boissonneault M, Houck A A, Schuster D I and Girvin S M 2008 *Phys. Rev. A* **77** 012112
- [45] Korotkov A N 1999 *Phys. Rev. B* **60** 5737
- [46] Korotkov A N *Quantum Bayesian Approach to Circuit QED Measurement* arXiv:1111.4016; see also ch 17 in Les Houches 2011 session XCVI on Quantum Machines
- [47] Wang P, Qin L and Li X Q 2014 *New J. Phys.* **16** 123047
- [48] Wang P, Qin L and Li X Q 2015 *New J. Phys.* **17** 059501
- [48] Feng W, Liang P, Qin L and Li X Q 2016 *Sci. Rep.* **6** 20492